

Quantumswitched heterojunction bistable bipolar transistor by chemical beam epitaxy

Ming C. Wu, Long Yang, and W. T. Tsang

Citation: [Applied Physics Letters](#) **57**, 150 (1990); doi: 10.1063/1.103968

View online: <http://dx.doi.org/10.1063/1.103968>

View Table of Contents: <http://scitation.aip.org/content/aip/journal/apl/57/2?ver=pdfcov>

Published by the [AIP Publishing](#)

Articles you may be interested in

[High stability heterojunction bipolar transistors with carbon-doped base grown by atomic layer chemical beam epitaxy](#)

J. Vac. Sci. Technol. B **14**, 3509 (1996); 10.1116/1.588789

[Commercial heterojunction bipolar transistor production by molecular beam epitaxy](#)

J. Vac. Sci. Technol. B **14**, 2216 (1996); 10.1116/1.588903

[Modeling and characteristics of bistable optoelectronic switches and heterojunction field effect transistors in molecular-beam epitaxially grown SiGe/Si](#)

J. Vac. Sci. Technol. B **11**, 1179 (1993); 10.1116/1.586836

[GaAs quantum well laser and heterojunction bipolar transistor integration using molecular beam epitaxial regrowth](#)

Appl. Phys. Lett. **59**, 2826 (1991); 10.1063/1.105872

[Quantumswitched heterojunction bipolar transistor](#)

Appl. Phys. Lett. **55**, 1771 (1989); 10.1063/1.102214



AIP | Journal of
Applied Physics

Journal of Applied Physics is pleased to
announce **André Anders** as its new Editor-in-Chief

Quantum-switched heterojunction bistable bipolar transistor by chemical beam epitaxy

Ming C. Wu, Long Yang, and W. T. Tsang
 AT&T Bell Laboratories, Murray Hill, New Jersey 07974

(Received 4 August 1989; accepted for publication 1 May 1990)

We proposed and demonstrated a novel bistable transistor—the quantum-switched heterojunction bistable bipolar transistor. The transistor has two current states. With increasing base-emitter voltage, the collector current is switched from *high* to *low*, while the base current is switched from *low* to *high*. Bistability is observed for a certain range of base voltage. This device has potential applications in implementing high-speed single bipolar transistor memories, gain quenching in light-emitting devices, and optoelectronic switching.

The bistable bipolar transistor has great potential for applications in high-speed single transistor memories and logic. Bistability has been obtained in negative differential resistance (NDR) bipolar and unipolar transistors by incorporating a resonant-tunneling double barrier (RTDB) in the base (gate) or between the base/emitter junction (gate/source).¹⁻⁷ The NDR in these transistors basically inherits from that of the RTDB. In this letter, we report the performance of a new bistable bipolar transistor—the *Q*-switched heterojunction bistable bipolar transistor (*Q*-switched HBBT). The single quantum well between a pair of thin barriers is placed in the center of the collector. The minimization of charge-storing wells makes it possible to operate at high speed. Bistability and switching between two current states were observed. The switching can be controlled by base potential. The present device has ON-OFF ratio of 3.5 for I_B , and 1.5 for I_C at 77 K. In the ON state (high collector current) it has a current gain of 35.

The schematic layer structure of the device is shown in Fig. 1. An InP/InGaAs/InP double barrier is inserted in the undoped collector of a double-heterojunction bipolar transistor (DHBT). The material was prepared by chemical beam epitaxy (CBE) on an n^+ -InP substrate. The details of the growth process have been reported elsewhere.⁸ The emitter and base consist of a 3000-Å-thick n -type InP layer ($N_D = 5 \times 10^{17} \text{ cm}^{-3}$) and a 1500-Å-thick p -type InGaAs layer ($N_A = 2 \times 10^{18} \text{ cm}^{-3}$), respectively. The collector consists of two parts: the first part is an n^- -doped InGaAs/InP (500 Å/600 Å) heterostructure, and the second part is formed by an InP/InGaAs/InP double barrier sandwiched between two 1000-Å-thick

undoped InGaAs layers. Both the well and the barriers of the double barrier are 100 Å thick.

A standard two-level mesa structure, as shown in Fig. 1, was used for electric contact and isolation. Typical emitter and base mesa areas are 2.5×10^{-5} and $1.9 \times 10^{-4} \text{ cm}^2$, respectively. The Ni/Ge/Au/Ag/Au was used for both emitter contact and backside collector contact, and AuBe/Ti/Au was used for the base contact. Sintering was done at 400 °C for 10 s.

The common-emitter current-voltage (I - V) characteristics at 77 K are shown in Fig. 2. Five traces are shown for different base voltages, starting at 1 V and increasing with a step of 70 mV. Unlike conventional HBTs, two collector turn-on voltages were clearly observed. For example, for $V_{BE} = 1.21 \text{ V}$ [trace (d)], the *Q*-switched HBBT is first turned on at $V_{CE} = V_{ON1} = 1.2 \text{ V}$. Then at $V_{CE} = V_{ON2} = 1.6 \text{ V}$, the collector current is switched abruptly to a high-current state. For $V_{CE} > V_{ON2}$, the collector current saturates well. A particularly interesting phenomenon is the hysteresis observed between the transition of the two states at V_{ON2} . This is believed to be caused by the space charges stored in the quantum well in the double barrier.⁹

When biased at constant collector voltage, the switching between the two current states can be controlled by the base voltage. Figure 3 shows the I_C and the I_B vs V_{BE} for

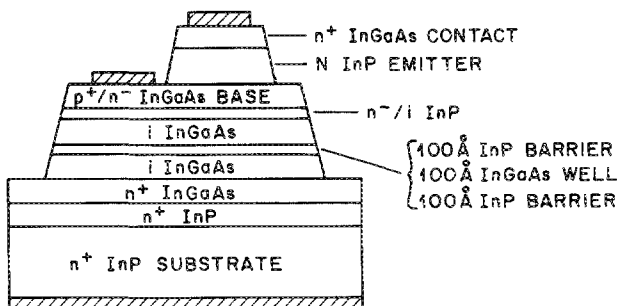


FIG. 1. Schematic structure of the InGaAs/InP *Q*-switched HBBT.

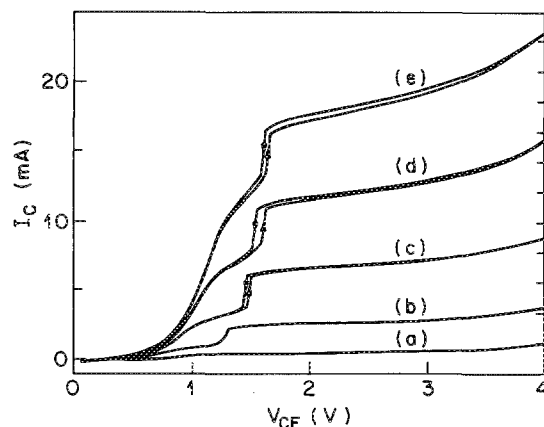


FIG. 2. Common-emitter I - V characteristics of the *Q*-switched HBBT at 77 K for $V_{BE} =$ (a) 1.00 V, (b) 1.07 V, (c) 1.14 V, (d) 1.21 V, and (e) 1.28 V. The emitter size is $2.5 \times 10^{-5} \text{ cm}^2$. The transistor has two sets of turn-on voltages, and bistability was observed at the second turn-on.

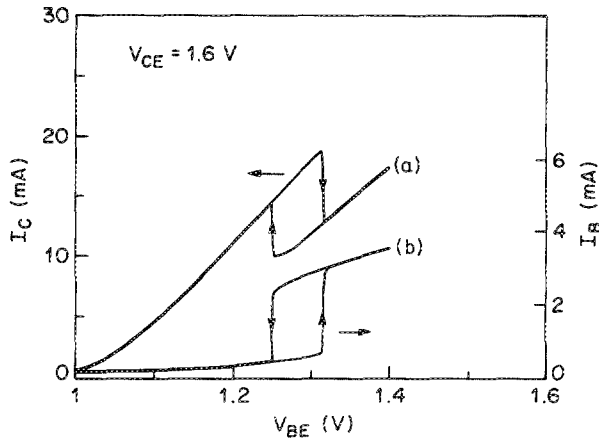


FIG. 3. Measured (a) collector current I_C and (b) base current I_B as functions of base voltage V_{BE} at $V_{CE} = 1.6$ V. Bistability is observed for $V_{BE} = 1.25$ – 1.32 V. It should be noted that I_B and I_C switch in the opposite direction.

$V_{CE} = 1.6$ V. Bistable operation is observed for V_{BE} between 1.25 and 1.32 V. Initially, I_C stays in the high-current state as V_{BE} increases from zero. As V_{BE} exceeds 1.32 V, I_C drops abruptly to the low-current state. When V_{BE} decreases, however, I_C does not switch back to high-current state until V_{BE} is less than 1.25 V. Another interesting phenomenon is the switching of the base current I_B . It switches in the opposite direction to I_C . The relation between I_C and I_B will be explained in more detail later. The ON-OFF ratios for I_C and I_B were 1.5 and 3.5, respectively, for the present device.

The physical mechanism of the switching can be understood qualitatively by the schematic band diagrams in Fig. 4. Figure 4(a) illustrates the band diagram of the transistor for $V_{CE} < V_{ON2}$. Because the transmission proba-

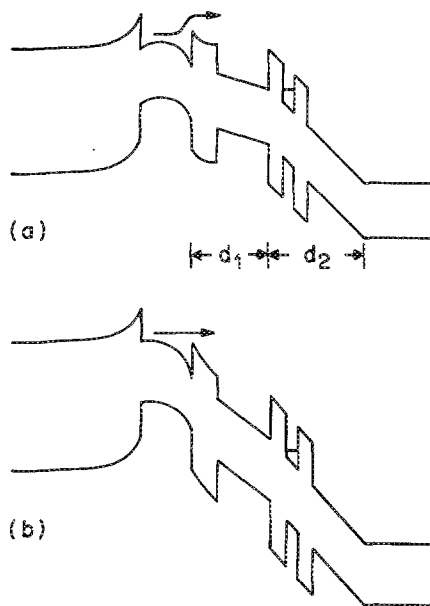


FIG. 4. Schematic band diagrams of the Q-switched HBBT (a) at the first turn-on and (b) after the second turn-on. In condition (a), the B/C barrier partially blocks electrons from entering the collector. In condition (b) that barrier is completely lowered and the electron transport efficiency through the base is greatly enhanced.

bility of the double barrier is small for small V_{CE} , space charges are accumulated in front of the double barrier. As a result, most V_{CB} drops between the double barrier and the collector contact. The base/collector (B/C) heterointerface barrier is not completely lowered and partially blocks electrons from entering the collector. The collector current is small in this case. On the other hand, the accumulated electrons in the base result in a large recombination component in the base current, as shown in Fig. 3 for $V_{BE} > 1.32$ V. As V_{CB} increases and reaches the resonance of the double barrier, a plateau shows up in the I_C vs V_{CE} plot (at V_{ON1} in Fig. 2). When V_{CE} reaches V_{ON2} , the B/C heterointerface barrier is completely lowered down, as shown in Fig. 4(b). The collector current increases abruptly because of a much improved electron transport efficiency through the base. The base current drops dramatically at the same time. This is because now electrons stop accumulating in the base, and the recombination component in the base current is greatly reduced.

A theoretical analysis is also performed using a simple model. The electric field and the distance between the B/C heterointerface and the double barrier are denoted by E_1 and d_1 , respectively, and those between the double barrier and the collector contact are denoted by E_2 and d_2 , respectively. For fixed V_{BE} , the current flowing through the B/C heterointerface, denoted by J_1 , depends on the B/C heterointerface barrier height, and thus the field E_1 , $J_1(E_1)$ is an exponentially increasing function when E_1 is below the critical field E_{1c} , at which the B/C heterointerface barrier is completely lowered down. It saturates for E_1 larger than E_{1c} . The current flowing through the double barrier can be modeled by

$$J_2 = \sigma T(E_2), \quad (1)$$

where σ is the sheet electron concentration in front of the double barrier, and T is the overall transmission probability through the double barrier. It has a peak corresponding to resonant tunneling and a subsequent increase due to thermionic emission. Neglecting the charges in the well, the sheet charge concentration in front of the double barrier is

$$\sigma = \epsilon \Delta E = \epsilon(E_2 - E_1), \quad (2)$$

where ϵ is the dielectric constant. Current continuity requires $J_1(E_1) = J_2(E_2)$, or

$$J_1(E_1) = \epsilon \left(\frac{d_1}{d_2} + 1 \right) \left(\frac{V'_{CB}}{d_1 + d_2} - E_1 \right) \times T \left(\frac{V'_{CB} - d_1 E_1}{d_2} \right), \quad (3)$$

where $V'_{CB} = d_1 E_1 + d_2 E_2$. Using explicit functions $J_1(E_1)$ and $T(E_2)$, Eq. (3) will determine the electric fields E_1 and E_2 , and the sheet charge concentration σ for any given V'_{CB} .

The calculated I_C vs V'_{CB} for a fixed V_{BE} is shown in Fig. 5(a), assuming that J_1 is dominated by thermionic emission. A moderate peak-to-valley ratio of 1.6 is used for the transmission probability T . (A current peak-to-valley ratio of 1.9 at 77 K was reported for similar InP/InGaAs/InP double barriers.¹⁰) Reasonable qualitative agreement

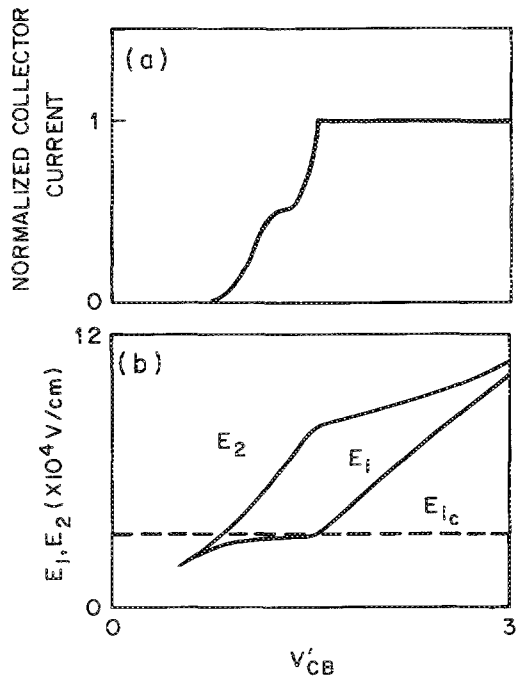


FIG. 5. Calculated collector current I_C vs V'_{CB} . (b) The calculated electric field vs V'_{CB} . The E_1 is the field between the B/C interface and the double barrier, whereas E_2 is the field between the double barrier and the collector contact. Both E_1 and E_2 vary nonlinearly with V'_{CB} .

with the experimental data is obtained. The experimentally observed second turn-on is more abrupt than that predicted theoretically, partly because the base recombination component of the injected electrons are now forced to enter the collector. Another reason is the feedback effect from the base resistance. The dramatic decrease of I_B at the second turn-on reduces the voltage drop across the base resistance. The intrinsic V_{BF} thus increases, causing more electrons to be injected from the emitter. The collector current does not decrease after the first turn-on (resonance of the double barrier) due to two reasons: first, the peak-to-valley ratio of the double barrier is small in the InP/InGaAs material system and second, the decrease in transmission probability T is partially compensated by the increase of the sheet charge concentration σ [see Eq. (1)]. The calculated electric fields E_1 and E_2 are shown in Fig. 5(b). Due to the space charges stored in the double-barrier region, both E_1 and E_2 vary nonlinearly with V'_{CB} . Before the second turn-on E_1 increases slowly toward the critical field E_{1c} , at which the B/C barrier is completely lowered. When E_1 exceeds E_{1c} , I_C increases rapidly and then saturates.

The Q -switched HBBT has potential applications in high-speed single bipolar transistor memory cells or flip flops. For example, if V_{BE} is biased inside the bistability loop of Fig. 3, the current state can be set by a negative V_{BE} pulse and reset by a positive V_{BE} pulse. A high-density static bipolar memory can thus be realized. Another interesting application is *gain quenching* in light-emitting devices. Before the second turn-on, the electrons and holes are confined by the DH and form efficient light-emitting sources, as in DH lasers or light-emitting diodes (LEDs).¹¹ The second turn-on lowers the B/C barrier, or equivalently, *quenches* the electron accumulation in the

base (see the switching of I_B in Fig. 3). The *optical gain* is thus quenched effectively. This is an intrinsically much faster process than the spontaneous recombination of carriers in conventional lasers or LEDs. With proper designs of the device geometries (for either lasers or LEDs), the Q -switched HBBT can also be used for optoelectronic switches because of the bistability of the radiative recombination current in I_B .

It is important to emphasize the differences between the Q -switched HBBT and the previously reported resonant-tunneling bipolar or hot-electron transistors. Those transistors incorporated a double-barrier resonant tunneling (DBRT) structure in the base, between base and emitter, or in the emitter. The double barrier's main function is controlling the injection of electrons from emitter. Base current and collector current usually switch in the same polarity. In Q -switched HBBT, the B/C heterointerface barrier height is most important in determining I_C . In addition, I_B and I_C switch in the opposite direction. The double barrier here is used to control the field distribution in the collector. The bistability comes from the space charges stored in the double barriers. By changing the position of the double barrier in the collector, the switching voltages can be designed to suit a particular application. Furthermore, the gain quenching of light-emitting device is a unique property of the Q -switched HBBT.

In conclusion, we have proposed and demonstrated a novel quantum-switched heterojunction bistable bipolar transistor. It has two current states: one with low collector current and high base recombination current, and the other one with high collector current and low base current. Bistable operation is observed for a certain range of base voltage. The switching can be controlled by the base potential. The present device has ON-OFF ratios of 1.5 and 3.5 for the collector and the base currents at 77 K, respectively. Theoretical study shows that larger ON-OFF ratios and room-temperature operation are possible with double barriers with higher current peak-to-valley ratios. The Q -switched HBBT has potential applications in high-speed single bipolar transistor memories, gain-quenched light-emitting devices, and optoelectronic switches.

- ¹F. Capasso and R. A. Kiehl, J. Appl. Phys. **58**, 1366 (1985).
- ²N. Yokoyama, K. Imaura, T. Mori, S. Hiyamizu, and H. Nishi, Jpn. J. Appl. Phys. **24**, L-853 (1985).
- ³F. Capasso, S. Sen, A. C. Gossard, A. L. Hutchinson, and J. H. English, IEEE Electron Device Lett. **EDL-7**, 573 (1986).
- ⁴K. Imamura, S. Muto, H. Ohnishi, T. Fujii, and N. Yokoyama, Electron. Lett. **23**, 870 (1987).
- ⁵T. Futatsugi, Y. Yamaguchi, S. Muto, N. Yokoyama, and A. Shibatomi, IEEE International Electron Device Meeting Technical Digest (IEEE, Washington, DC, 1987), p. 877.
- ⁶A. R. Bonnefoi, T. C. McGill, and R. D. Burnham, IEEE Electron Device Lett. **EDL-6**, 636 (1985); T. K. Woodward, T. C. McGill, and R. D. Burnham, Appl. Phys. Lett. **51**, 451 (1987).
- ⁷F. Capasso, S. Sen, and A. Y. Cho, Appl. Phys. Lett. **51**, 526 (1987).
- ⁸For a review, see W. T. Tsang, J. Cryst. Growth **81**, 261 (1987).
- ⁹V. J. Goldman and D. C. Tsui, Phys. Rev. Lett. **58**, 1256 (1987).
- ¹⁰T. H. H. Vuong, D. C. Tsui, and W. T. Tsang, Appl. Phys. Lett. **52**, 981 (1988).
- ¹¹See for example, H. C. Casey, Jr. and M. B. Panish, Heterostructure Lasers (Academic, Orlando, Florida, 1978).